© 2015. Published by The Company of Biologists Ltd | Journal of Cell Science (2015) 128, 4475-4486 doi:10.1242/jcs.173435

RESEARCH ARTICLE

The cytolinker plectin regulates nuclear mechanotransduction in keratinocytes

Filipe V. Almeida[1,2], Gernot Walko[3], James R. McMillan[4], John A. McGrath[5], Gerhard Wiche[6], Asa H. Barber[1] and John T. Connelly[2,*]

ABSTRACT

The transmission of mechanical forces to the nucleus is important for intracellular positioning, mitosis and cell motility, yet the contribution of specific components of the cytoskeleton to nuclear mechanotransduction remains unclear. In this study, we examine how crosstalk between the cytolinker plectin and F-actin controls keratin network organisation and the 3D nuclear morphology of keratinocytes. Using micro-patterned surfaces to precisely manipulate cell shape, we find that cell adhesion and spreading regulate the size and shape of the nucleus. Disruption of the keratin cytoskeleton through loss of plectin facilitated greater nuclear deformation, which depended on acto-myosin contractility. Nuclear morphology did not depend on direct linkage of the keratin cytoskeleton with the nuclear membrane, rather loss of plectin reduced keratin filament density around the nucleus. We further demonstrate that keratinocytes have abnormal nuclear morphologies in the epidermis of plectin-deficient, epidermolysis bullosa simplex patients. Taken together, our data demonstrate that plectin is an essential regulator of nuclear morphology *in vitro* and *in vivo* and protects the nucleus from mechanical deformation.

KEY WORDS: Keratinocyte, Mechanics, Nucleus, Keratin, Cyoskeleton, Plectin

INTRODUCTION

Mechanical and biophysical interactions between cells and their surrounding environment regulate essential processes, such as growth (Chen et al., 1997), survival (Chen et al., 1997), migration (Pelham and Wang, 1997) and differentiation (Connelly et al., 2010; Engler et al., 2006; McBeath et al., 2004), and in some instances contribute to disease progression (Paszek et al., 2005). Integrin-based adhesions and the actin cytoskeleton are classic physical linkages between cells and the extracellular matrix and regulate various aspects of cellular mechano-sensing (Dupont et al., 2011; Engler et al., 2006; McBeath et al., 2004). Nevertheless, how these intracellular structures transform mechanical forces into biochemical signals and influence cell behaviour remains unclear.

Recent evidence suggests that the nucleus itself might be a central mechano-sensing element within the cell. Expression levels of lamin A and lamin C (which are encoded by a single gene, *LMNA*, and hereafter are referred to as lamin A/C), a structural component of the nucleus, correlate with bulk tissue mechanics and, at a molecular level, mediate gene expression and stem cell differentiation (Swift et al., 2013). The nucleus also independently adapts to external forces through phosphorylation of the nuclear membrane protein emerin (Guilluy et al., 2014). Furthermore, chromatin has been proposed to undergo rapid conformational changes when an external mechanical stimulus is applied (Iyer et al., 2012). Thus, the transmission of forces to the nucleus might be a critical component of cellular mechanotransduction.

The nucleus physically connects to the cytoskeleton through the linker of nucleoskeleton and cytoskeleton (LINC) complex, which comprises nesprins, SUN1 and SUN2, and the nuclear lamina. The integrity of this linkage is essential for maintaining nuclear shape, structure and positioning within the cell (Gundersen and Worman, 2013; Isermann and Lammerding, 2013). Disruption of the LINC complex or the nuclear lamina leads to dramatic morphological changes in the nucleus (Lammerding et al., 2004), as well as defects in mitotic spindle orientation (Hale et al., 2008) and cell migration (Khatau et al., 2012; Lee et al., 2007; Zhang et al., 2009). Moreover, mutations in the genes encoding these structural proteins have been implicated in a variety of diseases, including progeria (Goldman et al., 2004), muscular dystrophy (Bonne et al., 1999) and deafness (Horn et al., 2013).

The nesprin family of proteins localise to the outer nuclear membrane and contain extra-nuclear domains that provide the first point of contact between the cytoskeleton and the nucleus (Zhang et al., 2001). Although the different nesprin chains interact with distinct components of the cytoskeleton, each has a conserved KASH domain that binds SUN1 and SUN2 within the inter-membrane space. SUN1 and SUN2 in turn bind to nuclear lamina proteins, thereby forming a continuous physical link between the cytoskeleton and the nucleoskeleton (Starr and Fridolfsson, 2010). Nesprin-1 and nesprin-2 giant bind to F-actin microfilaments (Zhang et al., 2001; Zhen et al., 2002), whereas nesprin-4 couples the nuclear membrane to microtubules through the kinesin-1 motor protein (Roux et al., 2009). Additionally, nesprin-3 connects to intermediate filaments through plectin (Wilhelmsen et al., 2005), a large (500 kDa) cytolinker that not only crosslinks intermediate filaments to each other, but also links them to the nuclear membrane, the actin cytoskeleton and integrin receptors (Castañón et al., 2013).

Whereas the actin cytoskeleton and LINC complex control nuclear mechanotransduction for some cell types (Li et al., 2014; Versaevel et al., 2012), the role of intermediate filaments in force transmission to the nucleus is less clear. In epidermal keratinocytes, the keratin cytoskeleton contributes substantially to overall cell rigidity and could potentially influence nuclear mechanotransduction (Kröger et al., 2013; Ramms et al., 2013; Seltmann et al., 2013). In this study, we investigated the mechanisms of force transmission to the nucleus in

[1]School of Engineering and Materials Science, Queen Mary, University of London, London, E1 4NS UK. [2]Centre for Cell Biology and Cutaneous Research, Barts and the London School of Medicine and Dentistry, Queen Mary, University of London, London, E1 2AT UK. [3]Centre for Stem Cells and Regenerative Medicine, King's College London, London, SE1 9RT UK. [4]The National Diagnostic EB Laboratory, Viapath, St Thomas' Hospital, London, SE1 7EH UK. [5]St John's Institute of Dermatology, King's College London (Guy's Campus), London, SE1 9RT UK. [6]Max F. Perutz Laboratories, Department of Biochemistry and Cell Biology, University of Vienna, 1030 Vienna, Austria.

*Author for correspondence (j.connelly@qmul.ac.uk)

Received 26 April 2015; Accepted 26 October 2015

Journal of Cell Science

Journal of Cell Science (2015) 128, 4475-4486 doi:10.1242/jcs.173435

keratinocytes using micro-patterned polymer substrates, which allow for precise control over single-cell adhesion and spreading. We demonstrate that cooperation between the cyto-linker, plectin and the actin cytoskeleton regulates nuclear deformation in response to defined biophysical cues. Furthermore, the nuclear morphology of keratinocytes in the epidermis of epidermolysis bullosa simplex (EBS) patients with plectin deficiency is perturbed. Taken together, our findings provide novel insights into the complex process of nuclear mechanotransduction and demonstrate a new function for plectin in epidermal keratinocytes.

RESULTS

Keratinocyte shape specifies nuclear morphology independently of acto-myosin contractility

To assess how cell shape affects the nuclear morphology of primary human keratinocytes, single cells were seeded onto micro-patterned collagen substrates of different sizes and shapes: circular islands of 20, 30 and 50 µm diameter and elliptical islands of shape factor 8 (SF8; the shape factor, denoted SF, is the ratio of the major axis to the minor axis) with an equivalent area to 30-µm diameter islands. The resultant 3D nuclear morphology was analysed by confocal microscopy 4 h after seeding when the cells on the larger islands were fully spread (Fig. 1A). The cross-sectional areas of the nuclei increased significantly as cells spread progressively on the 30 µm and 50 µm islands (Fig. 1B), whereas the height of the nucleus decreased slightly (Fig. 1C). Because the increase in area was proportionally greater than the decrease in height, cell spreading on the 50 µm islands resulted in an ∼40% increase in nuclear volume compared to cells on the 20 µm substrates (Fig. 1D). In addition to nuclear size, cell shape also correlated with nuclear shape. The nuclei of cells on the elliptical SF8 islands were more elongated, switching from oblate (disk-like) to prolate (zeppelin-like)

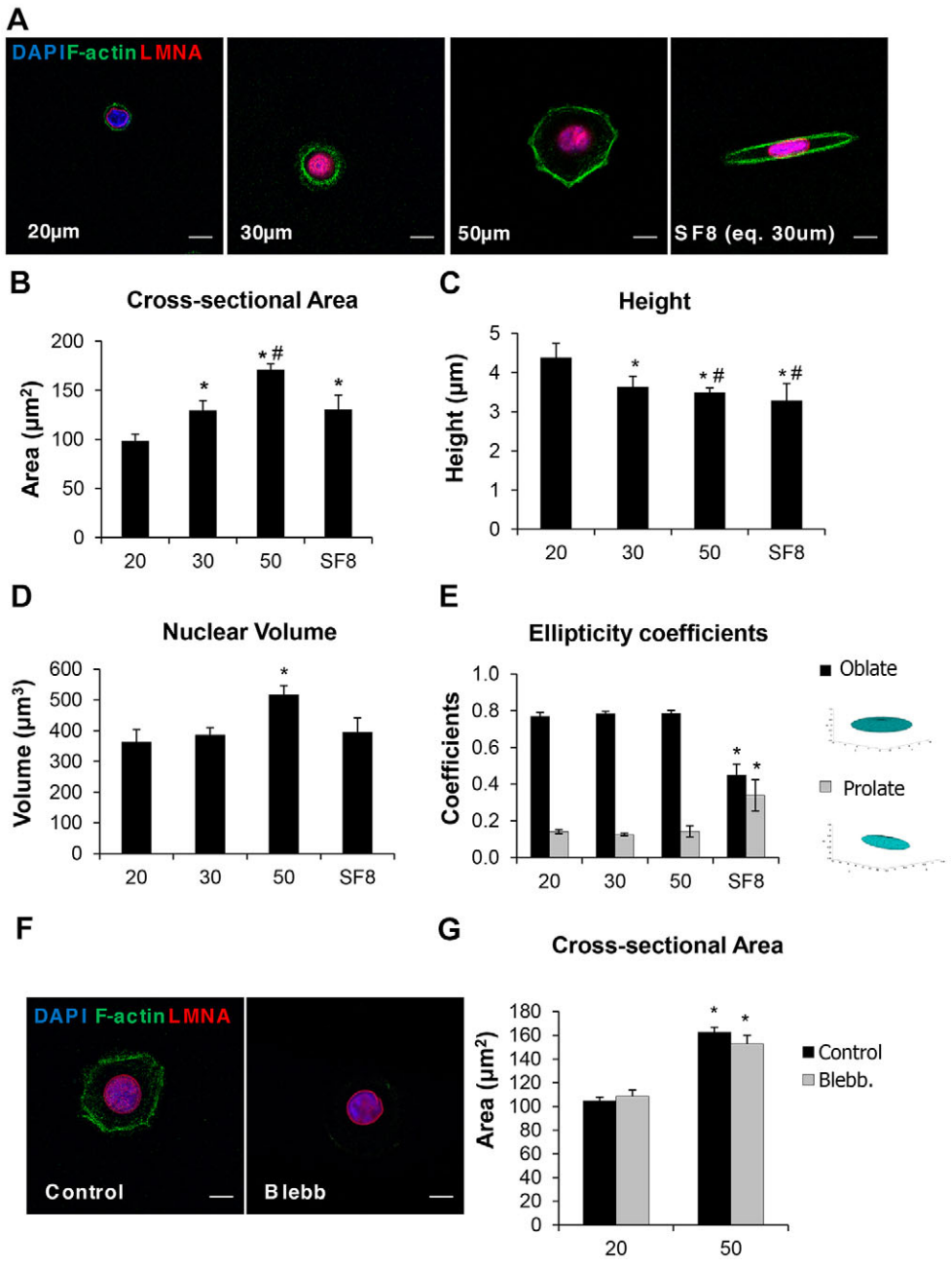

Fig. 1. Keratinocyte shape specifies 3D nuclear morphology. Primary human keratinocytes were cultured on either circular collagen islands with diameters of 20, 30 and 50 µm, or ellipses (SF8 with equivalent area of 30 µm). (A) Representative immunofluorescence images of F-actin (green), lamin A/C (red) and DAPI (blue) through the central plane of the cell were obtained by confocal microscopy. (B–E) Quantification of the maximum (B) cross-sectional area, (C) height, (D) volume and (E) geometrical shape coefficients was performed for cells on each of the micro-patterns using *z*-stacks of confocal images. (F) Representative confocal images of primary human keratinocytes cultured on 50-µm islands and treated with carrier (0.1% DMSO) or 50 µM blebbistatin. (G) Quantification of crosssectional area for experiments shown in F. Quantitative data represent mean±s.e.m. (n=3 experiments). *P<0.05 compared to 20 µm; §P<0.05 compared to 30 µm (one-way ANOVA). Scale bars: 10 µm.

Journal of Cell Science (2015) 128, 4475-4486 doi:10.1242/jcs.173435

ellipsoids, compared to cells on SF1 substrates (Fig. 1E). These results indicate that primary keratinocyte shape defines nuclear morphology, consistent with the response of other cell types (Li et al., 2014; Versaevel et al., 2012).

As the actin cytoskeleton is a key regulator of cell mechanics and directly links to the nucleus (Li et al., 2014; Zhen et al., 2002), we next investigated the role of cytoskeletal tension in cell-shape-induced nuclear deformation. To disrupt acto-myosin contractility, cells were treated with blebbistatin, which binds to the myosin II head domain and inhibits phosphate release (Kovács et al., 2004). Although blebbistatin completely blocked F-actin stress fibre formation, the cross-sectional areas of nuclei on 20 µm and 50 µm islands were unaffected (Fig. 1F,G). A similar response was observed in cells treated with the Rho-kinase inhibitor Y27632, and even complete disruption of actin polymerisation with latrunculin only partially blocked cell-shape-induced nuclear expansion on the 50-µm islands (Fig. S1A,B). We conclude that the actin cytoskeleton is not solely responsible for maintaining nuclear morphology in keratinocytes.

Plectin mediates cell-shape-induced nuclear deformation

The keratin network of intermediate filaments is a major structural and mechanical component of keratinocytes (Ramms et al., 2013; Seltmann et al., 2013). We therefore sought to determine how this cytoskeletal structure contributed to the regulation of nuclear morphology. We examined mouse keratinocytes lacking the gene for plectin (*Plec*), which controls keratin cytoskeletal organisation through non-covalent linkage of filaments (Castañón et al., 2013; Rezniczek et al., 1998; Steinböck et al., 2000). As previously described (Osmanagic-Myers et al., 2006), *Plec*-knockout (KO) keratinocytes had a more elongated, spindle-like morphology (Fig. 2A), and the keratin bundles were thicker and less dense

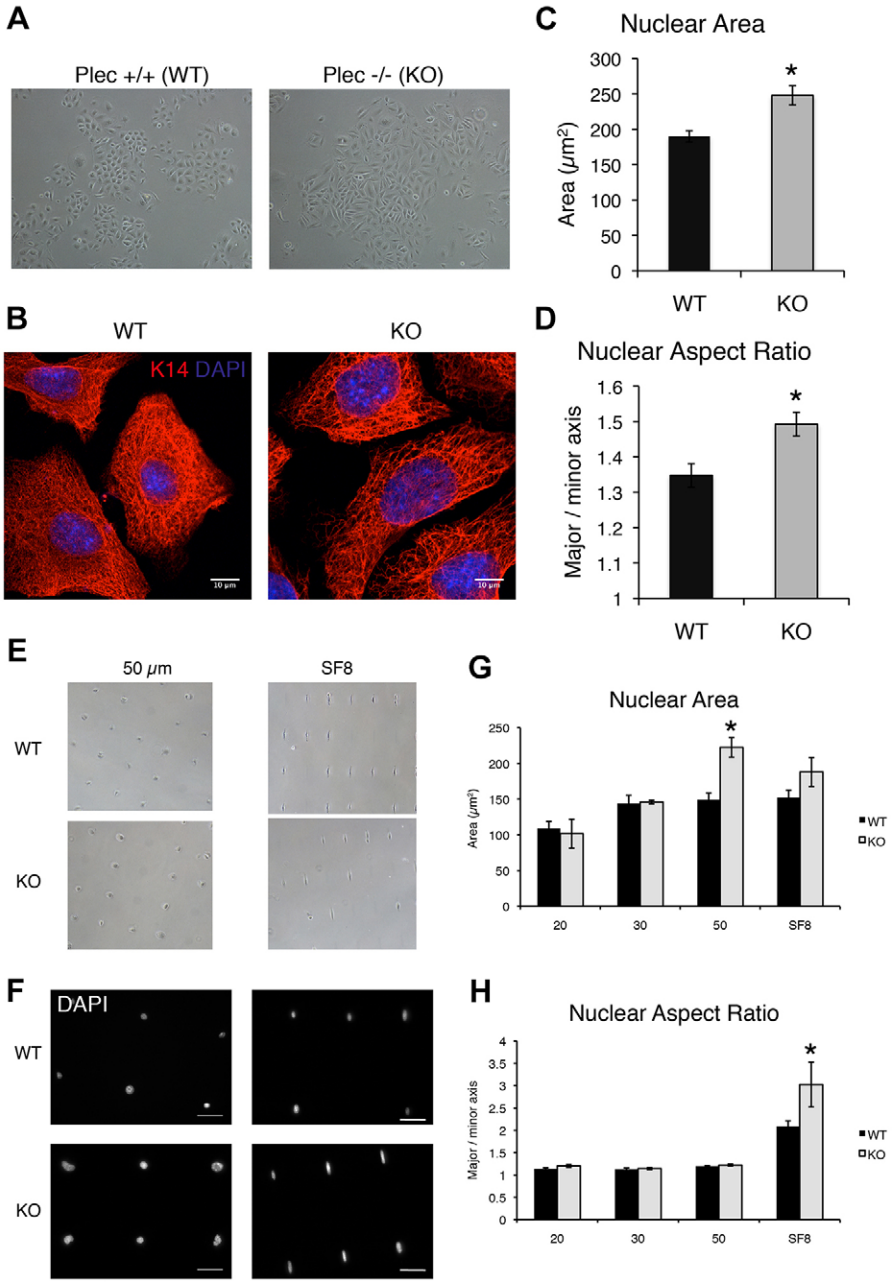

Fig. 2. Plectin mediates cell shape-induced nuclear deformation. (A) Representative bright field images of cell morphology for $Plec^{+/+}$ (WT) and $Plec^{-/-}$ (KO) keratinocytes. (B) Representative images of keratin 14 (K14) organisation and nuclear morphology (DAPI) of WT and KO cells. Scale bars: 10 µm. (C,D) Quantification of (C) nuclear cross-sectional area and (D) aspect ratio of WT and KO cells cultured on non-patterned surfaces. (E,F) Representative (E) bright field images and (F) DAPI fluorescence of WT and KO cells on 50 µm and SF8 micro-patterns. Scale bars: 50 µm. (G) Quantification of nuclear cross-sectional area and (H) aspect ratio of WT and KO cells on circular 20, 30 or 50 µm islands or SF8 islands. Quantitative data represent mean±s.e.m. (n=3 experiments). *P<0.05 compared to WT (one-way ANOVA).

Journal of Cell Science (2015) 128, 4475-4486 doi:10.1242/jcs.173435

compared to wild-type (WT) cells (Fig. 2B). Correlating with overall cell morphology on non-patterned surfaces, the nuclei of KO keratinocytes were significantly larger and more elongated than WT cells. We then analysed the nuclear morphology of WT and KO cells cultured on micro-patterned substrates to control for changes in cell shape and determine the direct effect of plectin on the nucleus. Like human keratinocytes, WT mouse cells displayed larger nuclei when allowed to spread on 50-µm islands and more-elongated nuclei on SF8 islands (Fig. 2E–H). The response to the micro-patterned surfaces was significantly more pronounced in *Plec*-KO cells, with nuclear area increasing from ~150 µm^2 to 220 µm^2 on the 50-µm substrates and the aspect ratio increasing from 2 to 3 on the SF8 substrates (Fig. 2E–H). The differences in nuclear area were observed within 4 h of seeding onto the patterned substrates and were sustained for up to 24 h (Fig. S2A). It is interesting to note that the level of nuclear deformation in KO cells was similar to that of HeLa cells, which express a different pattern of cytokeratins from epidermal keratinocytes (Moll et al., 1982) (Fig. S1). These findings indicate that in the absence of plectin, the nuclei of keratinocytes are more sensitive to extracellular physical cues and that plectin is a key regulator of nuclear morphology.

Crosstalk between plectin and acto-myosin contractility regulates keratin filament organisation and nuclear morphology

To understand the mechanism by which plectin regulates nuclear morphology, we next examined the organisation of various adhesive and cytoskeletal structures in WT and *Plec*-KO keratinocytes. KO cells displayed reduced staining for the hemidesmosomal integrin α6 (Fig. 3A), and more elongated focal adhesions, which appeared to associate with keratin filaments (Fig. 3B). Both WT and KO cells were competent to form actin stress fibres (Fig. 3C); however, the KO cells were more sensitive to inhibition of acto-myosin contractility with blebbistatin. In WT cells, treatment with blebbistatin reduced keratin bundle thickness, but the dense network structure was maintained (Fig. 3C). By contrast, treatment of KO cells with blebbistatin resulted in a dramatic collapse of the keratin network (Fig. 3C). These results suggest that cooperation between the actin and keratin cytoskeletons modulates keratinocyte structure and that the keratin network prevents a complete collapse of cell morphology even in the absence of acto-myosin tension.

To test whether crosstalk between actin and keratin also influences nuclear mechanics, we next examined the effects of blebbistatin on the nuclear morphology of WT and *Plec*-KO cells on micro-patterned substrates. Blebbistatin treatment abolished the differences in nuclear cross-sectional area and elongation on the 50-µm and SF8 micro-patterns, respectively (Fig. 4A–D). Thus, acto-myosin contractility is required for plectin-dependent changes in nuclear deformation. The reduced nuclear elongation caused by blebbistatin treatment (Fig. 4B,D) in particular suggests that tensile forces from the actin cytoskeleton promote nuclear deformation, and the more-pronounced elongation in KO cells (Fig. 4B,D) suggests that the keratin cytoskeleton opposes these forces and protects the nucleus from deformation.

The keratin cytoskeleton modulates nuclear morphology independently of direct linkage to the nuclear membrane

Plectin is a well-established cytolinker within the epidermis, and as demonstrated here and by others, it controls keratin filament organisation (Osmanagic-Myers et al., 2006). Plectin also connects intermediate filaments such as vimentin to the nuclear membrane through nesprin-3 (Wilhelmsen et al., 2005). Therefore, loss of plectin might potentially affect nuclear morphology either by disrupting the direct physical linkage and force transmission between the cytoskeleton and the nucleus or indirectly through changes in keratin structure and cellular mechanics. We examined

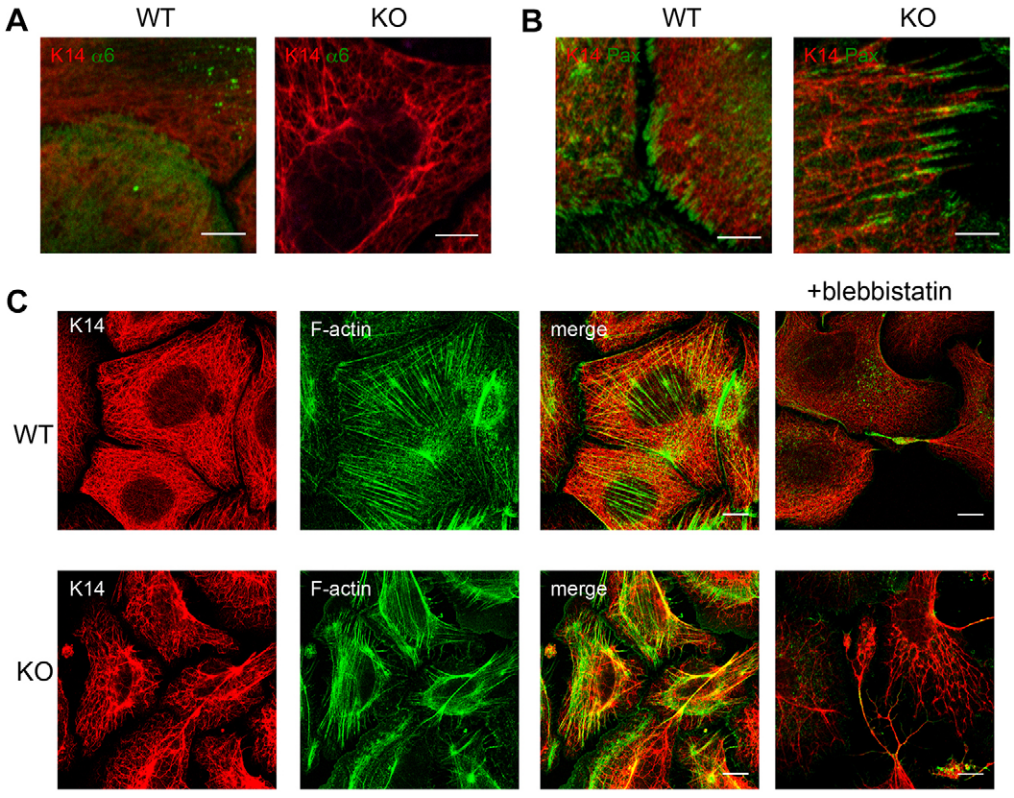

Fig. 3. Plectin regulates organisation of adhesive and cytoskeletal structures. Representative confocal immunofluorescence images of (A) keratin 14 (K14) and integrin α6 and (B) K14 and paxillin localisation in WT and *Plec*-KO keratinocytes. (C) K14 and F-actin images of WT and KO cells treated with carrier (0.1% DMSO) or 50 µM blebbistatin. Scale bars: 10 µm.

Journal of Cell Science (2015) 128, 4475-4486 doi:10.1242/jcs.173435

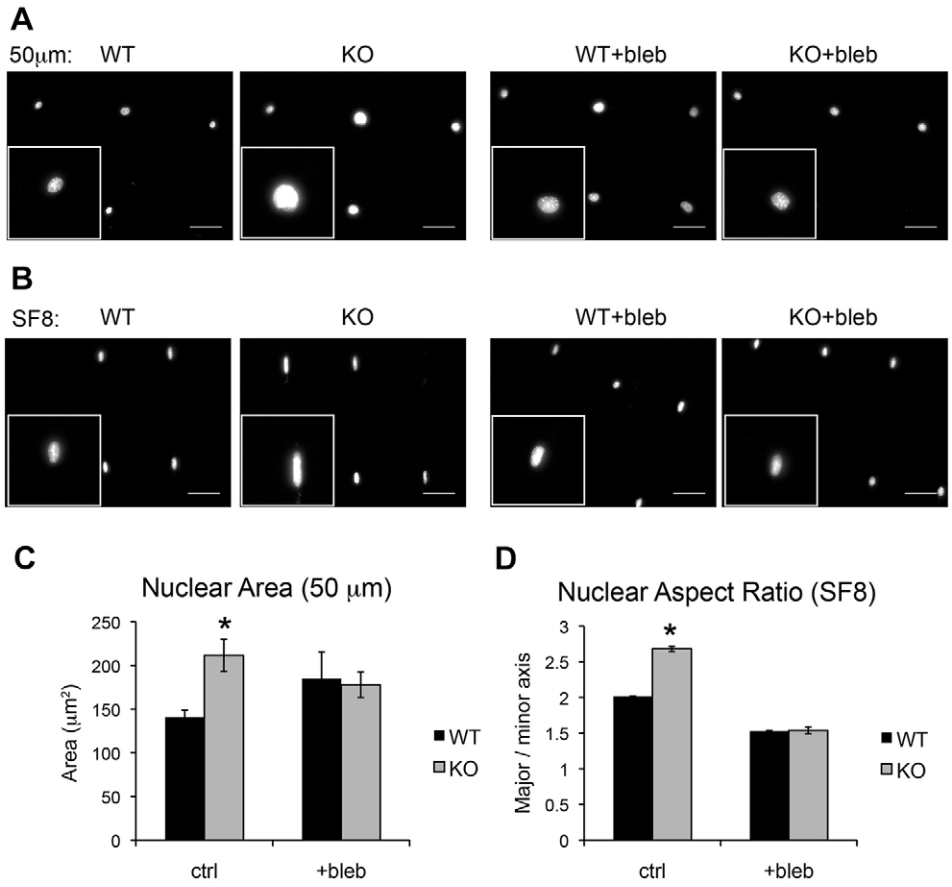

Fig. 4. Crosstalk between actin and keratin regulates nuclear morphology. Representative DAPI fluorescence images of WT and *Plec*-KO keratinocytes on (A) 50 µm and (B) SF8 micro-patterns. Cells were treated with carrier (0.1% DMSO) or 50 µM blebbistatin. Scale bars: 50 µm. Inset images are at a 2× magnification. (C) Quantification of nuclear cross-sectional area on 50 µm islands and (D) aspect ratio on SF8 patterns. Quantitative data represent mean±s.e.m. (n=3 experiments). *P<0.05 compared to WT (two-way ANOVA).

the expression and localisation of plectin and nesprin-3 in mouse keratinocytes. In WT cells, plectin colocalised with keratin filaments in the cytoplasm but not the nucleus, as would be expected based on its function as a cyto-linker (Osmanagic-Myers et al., 2006) (Fig. 5A). Similarly, diffuse nesprin-3 staining was only observed in the cytoplasm of WT keratinocytes, whereas in 3T3 fibroblasts it specifically localised to the nuclear membrane (Fig. 5B). Previous studies have demonstrated low nesprin-3 expression within the epidermis, and mice lacking nesprin-3 have a normal skin phenotype (Ketema et al., 2013). These findings suggest that in keratinocytes, plectin and nesprin-3 do not directly link keratins to the nuclear membrane.

To determine how disruption of nuclear–cytoskeletal linkages influences nuclear morphology in keratinocytes, we overexpressed a dominant-negative nesprin (DN-KASH), which comprises a KASH domain for localisation to the nuclear membrane but lacks any extranuclear cytoskeletal-binding domains (Zhang et al., 2001). Compared to GFP overexpression, DN-KASH had no effect on WT nuclei (Fig. 5C,D), which in conjunction with the immunofluorescence data, further supports an indirect role of plectin in nuclear mechanotransduction. Interestingly, DN-KASH expression in *Plec*-KO cells reduced nuclear area to WT levels (Fig. 5D). This effect might be due to disruption of the linkage between other nesprins (e.g. nesprin-1 and the nesprin-2 giant isoform) and the actin cytoskeleton, which is required for nuclear expansion in the absence of plectin.

Disulfide bonding of cysteine residues and serine/threonine phosphorylation are post-translational modifications involved in keratin filament assembly and organisation (Feng and Coulombe, 2015; Toivola et al., 2002). To gain further insight into how plectin deficiency affects keratin biochemistry and structure, we next performed western blot analysis of keratin 14 within the Triton-X-100-soluble and -insoluble fractions of cell lysates under both reducing and non-reducing conditions. In the soluble fraction, slightly increased keratin 14 could be observed in *Plec*-KO cells compared to WT cells under both reducing and non-reducing conditions, and there were decreased amounts of only the highest molecular mass keratin 14 species in the insoluble fraction of *Plec*-KO lysates under reducing conditions (Fig. 5E). Increased serine phosphorylation, which is associated with keratin solubility, was also observed in the cytoskeletal fraction of *Plec*-KO cells (Fig. 5F), and extracellular-related kinase 1/2 (ERK1/2, also known as MAPK3 and MAPK1) and p38 family proteins, upstream stimuli of keratin phosphorylation (Busch et al., 2012; Toivola et al., 2002), were required for plectin-dependent changes in nuclear area (Fig. S2B). Taken together, these results suggest that in addition to directly interacting with cytoskeletal components, plectin might also regulate nuclear morphology by mediating effects on keratin phosphorylation and filament stability.

Plectin dynamically mediates the effect of cell crowding on nuclear morphology

In addition to single-cell adhesion and spreading, we also sought to determine the role of plectin in regulating cell–cell interactions and nuclear morphology within multi-cell structures. WT and *Plec*-KO cells were seeded onto large micro-patterns of 200 µm in diameter at either low (37,500 per cm^2) or high (225,000 per cm^2) densities, and the 3D nuclear morphology was assessed by confocal microscopy. At low density (minimum to completely cover the micro-pattern), similar numbers of WT and KO cells

Journal of Cell Science (2015) 128, 4475-4486 doi:10.1242/jcs.173435

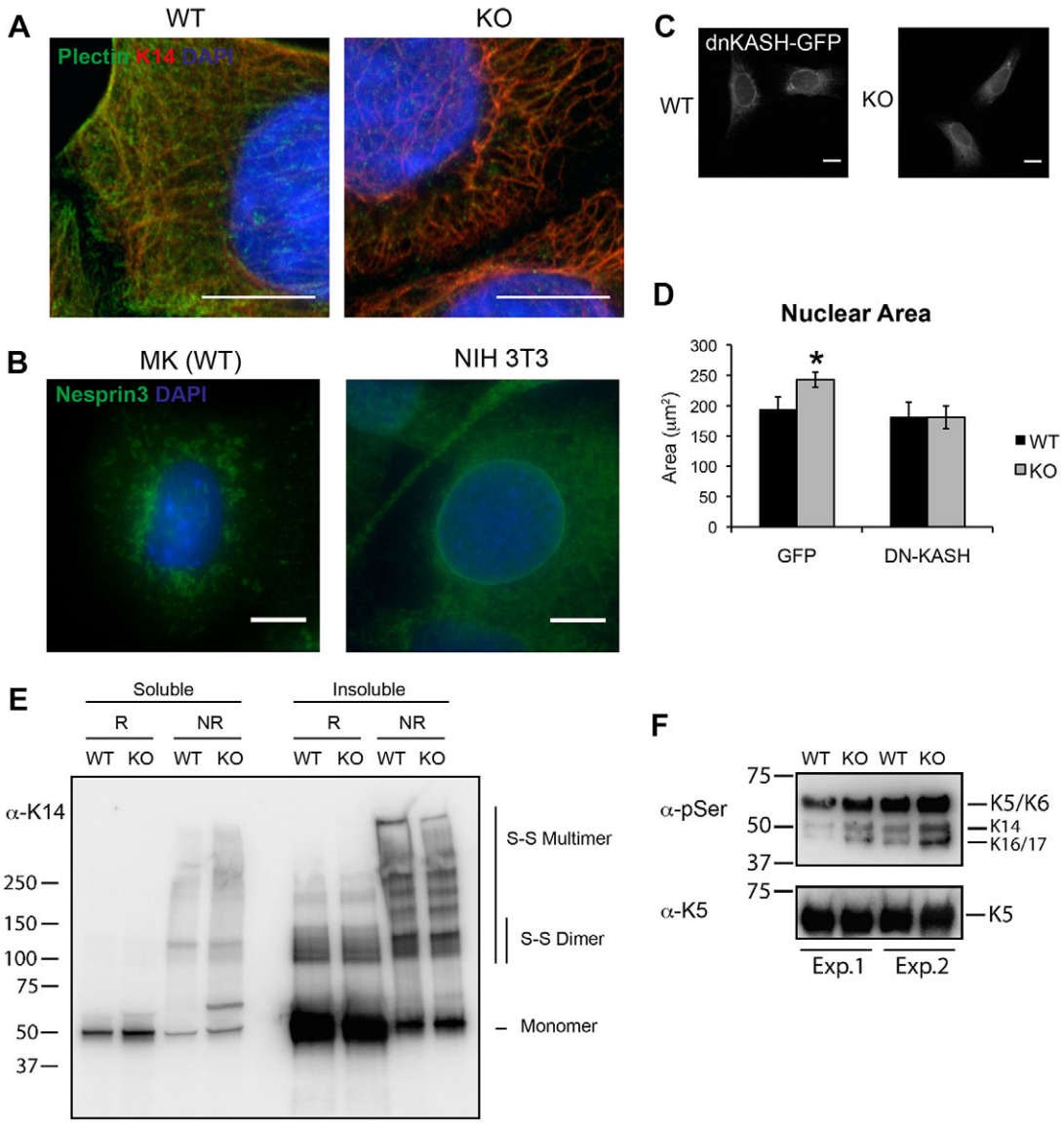

Fig. 5. Plectin regulates nuclear morphology independently of direct linkage to the nuclear membrane. (A) Immunofluorescence images of plectin, keratin 14 (K14) and DAPI localisation in WT and *Plec*-KO keratinocytes. (B) Immunofluorescence images of nesprin-3 and DAPI localisation in WT mouse keratinocytes and NIH 3T3 fibroblasts. (C) Fluorescent images of GFP-tagged dominant negative nesprin (dnKASH–GFP) expression in WT and KO keratinocytes. Scale bars: 10 µm. (D) Quantification of nuclear area in WT and KO cells transiently transfected with DN-KASH or GFP alone. All data represent mean±s.e.m. (n=3 experiments). *P<0.05 compared to WT (two-way ANOVA). (E) Western blot analysis of K14 in lysates from WT and KO keratinocytes separated into Triton-X-100-soluble and non-soluble fractions and run under reducing (R; with β-mercaptoethanol) or non-reducing (NR) conditions. (F) Western blot analysis of serine phosphorylation (pSer) and keratin 5 (K5) in insoluble cytoskeletal fractions of WT and KO lysates under reducing conditions.

adhered to the patterns, and the nuclei of the KO cells were significantly larger than WT (Fig. 6A–C), consistent with the single-cell experiments. When seeded at high density, however, there were significantly more KO cells per micro-patterned island than WT cells. The nuclear volume of KO cells at high density was also significantly smaller than at low density, whereas the seeding density had no effect on the nuclear volume of WT cells. Intriguingly, the nuclei of the KO cells were more elongated in the apical direction (z-axis) compared to the WT cells at both densities (Fig. 6D,E). These results indicate that plectin is important for cell density sensing. In the absence of plectin, keratinocytes are more sensitive to cell crowding, which in turn affects cell packing and nuclear deformation, and might reflect defects in the keratin cytoskeleton and cellular mechanics.

To investigate the plasticity and dynamics of nuclear deformation, we next took advantage of dynamically adhesive micro-patterns developed in our laboratory (Costa et al., 2014), and investigated nuclear morphology when keratinocytes were released from the micro-patterns and induced to migrate. Cells were seeded onto 200-µm islands at high density for 12 h, then activated to migrate by functionalisation of the surrounding polymer brushes with a collagen mimetic peptide (Reyes and García, 2003) (Fig. 6F). Nuclear cross-sectional area remained relatively constant in WT cells migrating onto the functionalised surfaces, whereas the nuclear area increased significantly in *Plec*-KO cells within 6 h of activation (Fig. 6G). These results demonstrate that reduced nuclear area caused by cell crowding in KO cells is reversible, and the nuclei expand again when cells are allowed to migrate and spread.

Journal of Cell Science (2015) 128, 4475-4486 doi:10.1242/jcs.173435

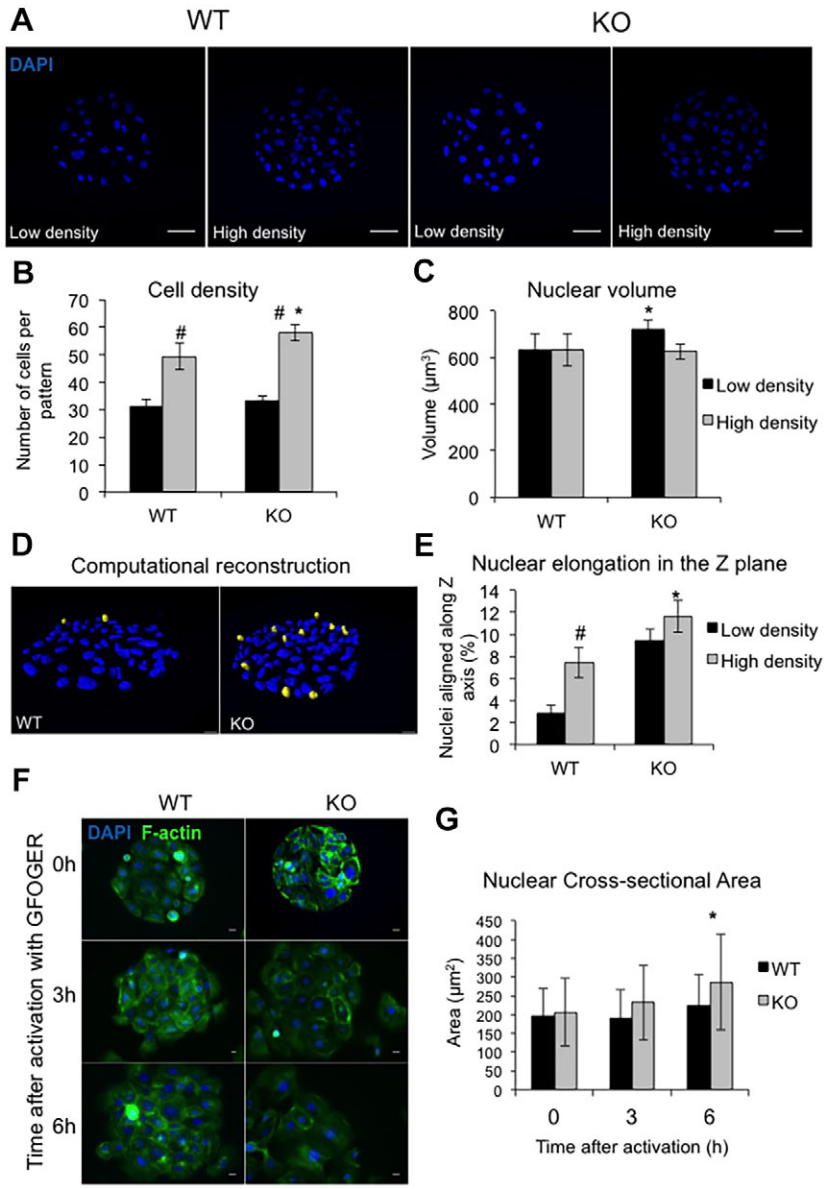

Fig. 6. Plectin influences cell crowding and nuclear morphology in multi-cell structures. (A) Representative confocal images of DAPI-stained WT and *Plec*-KO cells seeded on 200-μm islands at low (37,500 per cm^2) and high (225,000 per cm^2) densities. Scale bars: 50 μm. (B,C) Quantification of (B) the number of nuclei per pattern and (C) nuclear volume. (D) Representative 3D reconstruction of DAPI-stained nuclei. Yellow nuclei show those preferentially aligned with the *z*-axis. (E) Quantification of the percentage of nuclei preferentially elongated in the *z*-axis (angle of major axis 45° above *x*-*y* plane). Data represent mean±s.e.m. (n=3 experiments). *P<0.05 comparing WT versus KO; $^{\psi}P$<0.05 comparing low versus high density seeding (two-way ANOVA). (F) Representative fluorescence images of F-actin and DNA of WT and KO cells before (0 h) and 3 and 6 h after photo-activated coupling of the collagen-mimetic peptide (GFOGER) to the surrounding polymer surface. Scale bars: 10 μm. (G) Quantification of nuclear morphology at 0, 3 and 6 h after activation with the GFOGER peptide. Data represent the mean±s.d. (n>72 cells) of a representative experiment. *P<0.05 comparing WT and KO at 6 h (two-way ANOVA).

Nuclear morphology is perturbed in the epidermis of EBS-MD patients

In human skin, mutations in the *PLEC* gene cause the blistering disease epidermolysis bullosa simplex with muscular dystrophy (EBS-MD) (McLean et al., 1996; Smith et al., 1996; Winter and Wiche, 2013). To investigate whether plectin also influences nuclear mechanics *in vivo*, we analysed the morphology of nuclei in the epidermis of four EBS-MD patients with confirmed plectin deficiency (Table S1). Compared to normal epidermis, the nuclei of basal keratinocytes in the EBS-MD samples were significantly smaller, less circular and elongated in the apical direction (Fig. 7A–D), and these differences occurred independently of cell proliferation (Fig. S3). These findings demonstrate that plectin also regulates the nuclear morphology of human keratinocytes *in vivo*. The more apically elongated nuclei observed in the EBS-MD samples are consistent with the *in vitro* effects of cell crowding and previously reported changes in the nuclei of *Krt14*-KO mice (Lee et al., 2012). Thus, our data suggest that *PLEC* mutations might directly influence nuclear morphology within the epidermis through changes in keratin structure and cellular mechanics.

DISCUSSION

In this study, we examined the mechanisms of force transmission from external adhesive cues to the nucleus of epidermal keratinocytes. We took advantage of micro-patterned collagen substrates to precisely control the adhesion and spreading of single cells, as well as crowding in multi-cell clusters. Our results demonstrate that in keratinocytes, the size and shape of the nucleus changes in response to defined biophysical cues, and the extent of this deformation is controlled by crosstalk between plectin and acto-myosin contractility. Plectin is required for maintaining a dense keratin network and dampens nuclear deformation induced by either cell spreading or crowding (Fig. 8). Interestingly, this effect does not appear to involve direct linkage of plectin to the nuclear membrane. Based on these findings, we propose a model in which the keratin cytoskeleton provides a rigid network that resists both tensile and compressive forces imposed on the cell and protects the nucleus from excessive deformation.

Plectin is a well-established regulator of cytoskeletal architecture across different cell types. Consistent with our findings, the absence of plectin in keratinocytes induces the formation of thicker keratin

Journal of Cell Science (2015) 128, 4475-4486 doi:10.1242/jcs.173435

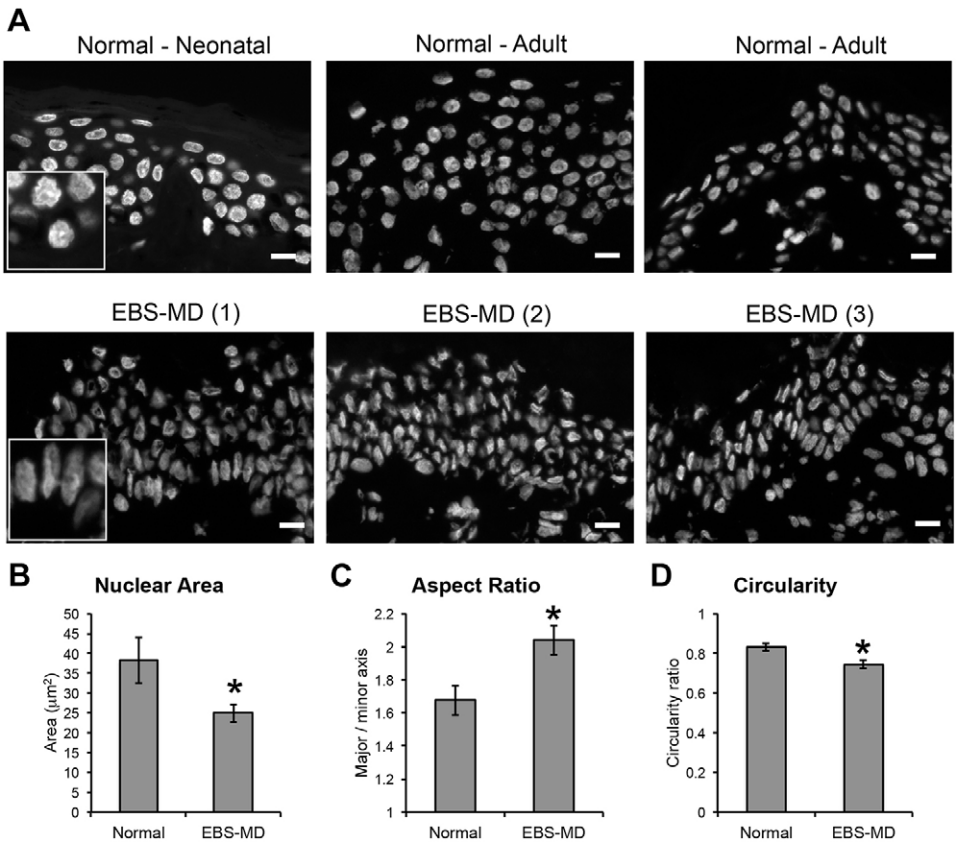

Fig. 7. Nuclear morphology is perturbed in plectin deficient epidermis. (A) Representative images of DAPI-stained frozen sections from biopsies of normal neonatal and adult and EBS-MD skin. Scale bars: 10 µm. Inset images are at 2× magnification. (B–D) Quantification of (B) nuclear cross-sectional area, (C) aspect ratio and (D) circularity of basal keratinocytes. At least 100 cells were measured per specimen. Data represent the mean±s.e.m. (n=4 patients). *P<0.05 compared to normal skin (one-way ANOVA).

bundles, with noticeably larger voids within the meshwork (Osmanagic-Myers et al., 2006). Loss of plectin in keratinocytes also increases MAPK activity and enhances cell migration (Osmanagic-Myers et al., 2006). However, this response appears to be specific to the cell type. In fibroblasts, plectin is necessary for localisation of vimentin intermediate filaments to focal adhesions at the cell periphery (Burgstaller et al., 2010; Spurny et al., 2008) and inhibits cell motility (Gregor et al., 2014). MCF-7 breast cancer cells similarly acquire a slower, less-protrusive phenotype in the absence of plectin (Boczonadi et al., 2007). Plectin also affects the organisation of the intermediate filament protein glial fibrillary acidic protein (GFAP) in astrocytes, and contributes to the fibrotic phenotype of R239C GFAP mutant cells (Tian et al., 2006). Finally, loss of plectin reduces fibroblast stiffness and impairs force transmission (Na et al., 2009). Thus, plectin is a key regulator of cellular mechanics, and our data add a new dimension to this function, specifically in the control of nuclear morphology.

Here, we provide evidence that plectin indirectly protects the nucleus from deformation owing to altered keratin structure rather than direct linkage to the nuclear membrane. Recent studies have shown that disulfide bonding of cysteine residues within keratin 14 molecules are important for the maturation of the perinuclear keratin network, which in turn limits nuclear movement (Feng and Coulombe, 2015; Lee et al., 2012). Consistent with these reports,

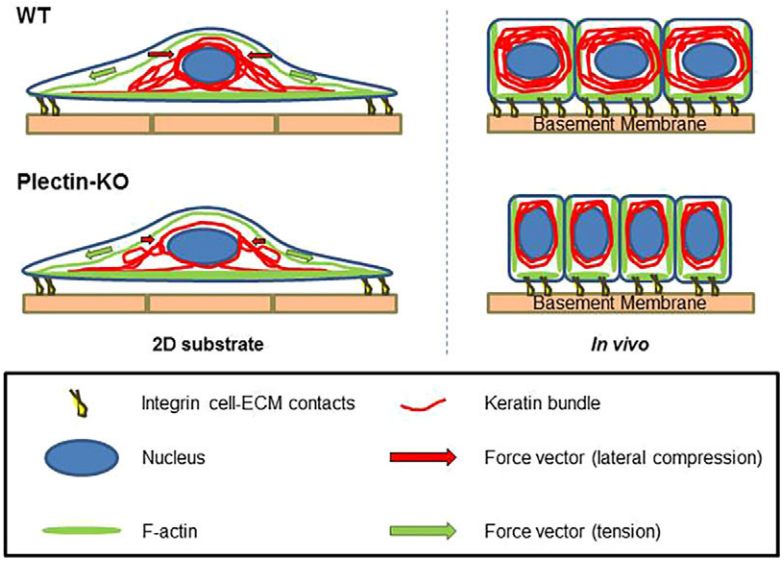

Fig. 8. Proposed model for the role of plectin in nuclear mechanotransduction. In the presence of plectin, a dense, cross-linked keratin network protects the nucleus of keratinocytes from excess expansion during cell spreading (e.g. on single-cell micro-patterns), whereas at high cell density (e.g. *in vivo*) nuclei are resistant to lateral forces from adjacent cells. Plectin deficiency therefore causes increased nuclear deformation in response to both tensile and compressive forces.

Journal of Cell Science (2015) 128, 4475-4486 doi:10.1242/jcs.173435

our data suggest that loss of plectin might slightly inhibit the assembly of high-molecular-mass keratin 14 species, thereby weakening the structure of keratins around the nucleus and further increasing the susceptibility to mechanical deformation. However, the main effect of plectin on nuclear deformation likely results from stabilisation of the keratin network by non-covalently linking filaments to each other and to other cytoskeletal components. Beyond keratins, other intermediate filaments, such as lamin A/C, are also key regulators of nuclear morphology (Wang et al., 2008) and cell function within the epidermis (Sagelius et al., 2008). How the various cytoskeletal structures around the nucleus mechanically integrate and depend on specific post-translational modifications will be an important consideration for future studies.

The effects of plectin deficiency might not simply be due to altered cellular mechanics. MAPK activity is elevated in *Plec*-KO keratinocytes (Osmanagic-Myers et al., 2006), and our data further demonstrate that MAPK signalling is required for changes in nuclear area. Both p38 family proteins and ERK1/2 promote keratin phosphorylation (Busch et al., 2012; Toivola et al., 2002), which might regulate nuclear morphology through changes in keratin solubility. However, these kinases affect many signalling pathways and might regulate nuclear morphology through additional mechanisms. Increased inflammation or cellular stress in the fragile skin of plectin-deficient patients could similarly contribute to altered nuclear morphology, independently of cytoskeletal mechanics.

Although plectin clearly regulates keratinocyte nuclear morphology, the direct impact on cell behaviour and disease progression is still to be determined. Changes in the size and shape of the nucleus could potentially affect chromatin structure and gene expression. Our previous studies have shown that when cell spreading is restricted on small micro-patterns, keratinocytes decrease their rate of proliferation and increase terminal differentiation, which is mediated by serum response factor and AP-1 transcriptional activity (Connelly et al., 2010). In addition, histone de-acetylation correlates with decreased cell spreading, reduced nuclear size and terminal differentiation on micro-patterned substrates (Connelly et al., 2011). During terminal differentiation in the mouse epidermis, increased clusters of heterochromatin accompany decreased nuclear volume (Gdula et al., 2013), and regulators of nuclear architecture and chromatin remodelling, such as Ezh2, Satb1 and Brg1, are required for positioning and expression of genes within the epidermal differentiation complex (EDC) (Botchkarev et al., 2012; Ezhkova et al., 2009; Fessing et al., 2011; Mardaryev et al., 2014). Thus, decreased nuclear volume on small micro-patterns might facilitate terminal differentiation by physically forcing chromatin condensation. In other cell types, such as embryonic stem cells, chromatin de-condensation follows nuclear softening (Chalut et al., 2012), and direct mechanical stimulation of HeLa cells causes rapid de-compaction of chromatin (Iyer et al., 2012). Although there is strong evidence that nuclear mechanics might directly regulate chromatin remodelling, gene expression and cell behaviour, a definitive causative relationship has yet to be established.

Clinically, mutations in plectin (plectinopathies) manifest as different symptoms according to the specific isoforms (Winter and Wiche, 2013), whereas mutations in keratin 5 and 14 themselves disrupt keratin filament mechanics (Russell et al., 2004) and lead to distinct forms of EBS (Coulombe et al., 1991). In future studies, investigation of how other types of plectin mutations, such as in EBS Ogna (Walko et al., 2011), and EBS caused by keratin mutations affect nuclear morphology and gene expression will be of great importance. Recent mRNA expression profiling studies, implicating pathways related to interleukins, lipid metabolism and keratinisation, suggest that transcriptional mechanisms might indeed play a role in EBS (Bchetnia et al., 2012; Lu et al., 2007). Ultimately, identifying the impact of altered nuclear mechanics in the pathophysiology of blistering skin diseases could shed new light on our understanding and treatment of these complex and painful conditions.

MATERIALS AND METHODS

Fabrication of micro-patterned substrates

In order to control adhesive area, patterned polymerised (oligo ethylene glycol methacrylate; POEGMA) brushes were used. Briefly, master silicon moulds were created by photolithography and used to cast poly-dimethylsiloxane stamps. The micro-patterned stamps were inked with the thiol initiator ω-mercaptoundecyl bromoisobutyrate and brought into conformal contact with gold-coated coverslips for 15 s to deposit the initiator as a self-assembled monolayer. Atom transfer radical polymerisation (ATRP) of the monomeric solution oligo(ethylene glycol) methacrylate (OEGMA; M_n 360 for -OH brushes) and oligo(ethylene glycol) methyl ether methacrylate (M_n 300 for -CH_3-terminated brushes), was carried out in a water:ethanol (4:1) solution of OEGMA (1.6 M), Cu(II) Br (3.3 mM), 2,2-bipyridine (82 mM) and Cu(I)Cl (33 mM). The reaction was performed at room temperature from 0.25–1 h. For dynamically adhesive micro-patterns, substrates were further modified with alkyne moieties as previously described (Costa et al., 2014). Following sterilisation with 70% ethanol, patterned substrates were coated with 20 µg/ml of rat type I collagen (BD Biosciences) in PBS for 1 h at 37°C. Substrates were rinsed three times with 1 mM HCl and twice with PBS. All chemicals were from Sigma-Aldrich unless otherwise indicated.

Cell culture

Primary human keratinocytes were isolated from neonatal foreskin and maintained on a feeder layer of J2 3T3 fibroblasts, as previously described (Rheinwald and Green, 1977). Cells were cultured in FAD medium containing 1 part Ham's F12 (Life Technologies), 3 parts Dulbecco's modified Eagle's medium (DMEM; Life Technologies), 10^{-4} M adenine, 10% FBS (Biosera), 1% penicillin-streptomycin (Life Technologies), 0.5 µg/ml hydrocortisone, 5 µg/ml insulin, 10^{-10} M cholera toxin and 10 ng/ml EGF (Peprotech). Immortalised *Plec*$^{-/-}$ and *Plec*$^{+/+}$ mouse keratinocyte cell cultures were established from Plec$^{-/-}$/p53$^{-/-}$ and Plec$^{+/+}$/p53$^{-/-}$ mice, as previously described (Andrä et al., 2003) and maintained in EpiLife medium with human keratinocyte growth supplement (Life Technologies). NIH 3T3 cells were maintained in DMEM supplemented with 10% fetal bovine serum (FBS) and 1% penicillin-streptomycin. For seeding onto micro-patterned substrates, regardless the type of substrate, both primary human and mouse keratinocytes were trypsinised (passages ranging 2–8 for the primary human keratinocytes and 8–18 for the mouse keratinocytes) and re-seeded onto the micro-patterned substrates at varying densities ranging from 10,000 to 25,000 cells/cm^2. Cells were allowed to adhere for 0.5–1 h and then rinsed three times with fresh medium. Where indicated, cells were treated for 3 h with 50 µM blebbistatin (Merck Millipore), 1 µM latrunculin (Merck Millipore), 10 µM Y27632 (Merck Millipore) or carrier control (0.1% DMSO). To activate cell migration out of the micro-patterns, substrates were functionalised with a collagen mimetic peptide containing the GFOGER motif (Reyes and García, 2003) (Activotec). Cells were exposed to 1 mg/ml GFOGER in phenol-free DMEM containing 0.5% Irgacure 2959. The coupling reaction was initiated by exposure to 365-nm light from an LED array (Cetoni, Germany) for 1 min. After exposure, substrates were immediately washed three times with DMEM.

EB skin samples

Plectin deficient EBS-MD and control skin biopsies were provided by the EB Laboratory at St Thomas' Hospital (Viapath, London). Ethical approval was obtained from Guy's and St Thomas' NHS Trust Research Ethics committee, code 07/H0802/104 (primary investigator, John A McGrath),

with all experiments conducted according to the Declaration of Helsinki. Following informed consent, a shave biopsy of normal-appearing, rubbed skin was taken from the arm or thigh following local anaesthetic with 2% lignocaine. Skin biopsies were transported to the EB Laboratory where they were washed on a rotator in PBS at 4°C. Samples were then embedded and mounted in Tissue-Tek® OCT compound (Agar Scientific) and snap frozen in liquid nitrogen-cooled n-heptane for storage at −80°C until 5–7-µm cryostat skin sections were cut using a Bright OTF500 cryostat (Bright Instruments). Plectin-deficient samples were previously identified by the EB Laboratory by negative staining with at least two out of six anti-plectin diagnostic antibodies.

Plasmids and transfection

Mouse keratinocytes were cultured in Epi-life medium for 24 h prior to transfection. Cells were transfected for 3 h using 1 µl Lipofectamine 2000 (Life Technologies) and 1 µg of DNA per 10^5 cells. The dominant-negative nesprin (DN-KASH) construct was kindly provided by Derek Warren (King's College London, London, UK) and has been described previously (Zhang et al., 2001).

Immunofluorescence imaging and quantification

For immunofluorescence microscopy, cells were fixed with 4% paraformaldehyde (PFA) and permeabilised with 0.2% Triton X-100 in PBS for 10 min at room temperature and washed three times in PBS. Samples were blocked for 1 h in 10% bovine serum plus 0.25% fish gelatin, incubated with primary antibodies for 1 h at room temperature or at 4°C overnight, and incubated with secondary antibodies (Life Technologies, 1:1000) for 1 h at room temperature. Samples were mounted on glass slides with Mowiol reagent. Primary antibodies were against the following: lamin A/C (Santa Cruz Biotechnology, Ms 636, 1:200), K14 (Cancer Research UK, Ms LL002, 1:500), K14 (Covance, Rb polyclonal, 1:5000), α6 integrin (BD Biosciences, Rat GoH3, 1:100), paxillin (BD Biosciences, Ms 177, 1:200), plectin (Ms 10F6, 1:2) (Walko et al., 2011) and nesprin-3 (gift from Arnoud Sonnenberg, Netherlands Cancer Institute, Amsterdam, The Netherlands; rabbit polyclonal, 1:100). F-actin was labelled with phalloidin–Alexa-Fluor-488 (Life Technologies, 1:500).

High-resolution images were acquired with either a Zeiss 510 or 710 confocal microscope. For low-magnification epi-fluorescence microscopy, either a Leica DMI4000 or Leica DMI5000 microscope was used. ImageJ was used for two-dimensional data analysis of epi-fluorescent images. For the processing and analysis of *z*-stacks of single cells, a MatLab (MathWorks) script was developed. Briefly, each frame was threshold using Otsu's method. As the pixel area through the *z*-stacks followed a normal distribution, the height was determined by counting the frames resembling a pixel area superior within $\mu \pm 0.64\sigma^2$ of the fitted Gaussian curve. For the quantification of 3D geometry, Imaris (Bitplane) was used to fit an ellipsoid to the DAPI signal and calculate volume, ellipticity (both prolate and oblate) and *x*-*y*-*z* axes (both absolute and normalised lengths). To determine whether the nucleus was oriented in the apical or lateral direction, the sine of the angle between the major axis of the fitted ellipsoid (*c* axis) and the *x*-*y* plane was calculated. Nuclei oriented in the apical direction were defined as having angles above 45° [sin (Ø)≈0.71 of normalised vector].

Western blot analysis

Equal numbers of plectin-KO and WT keratinocytes were first lysed in cold Triton X-100 lysis buffer (1% Triton X-100, 0.5% NP-40, 150 mM NaCl, 20 mM Tris-HCl, 1 mM EDTA and supplemented with PhosSTOP® Phosphatase Inhibitor and cOmplete® EDTA-free Protease Inhibitor Cocktails (Roche) for 30 min (4°C), and detergent-soluble and -insoluble proteins were separated by centrifugation (16,000 ***g*** for 20 min at 4°C). Detergent-insoluble proteins were then dissolved in the same volume of radio-immune precipitation assay (RIPA) buffer (no reducing agent) containing 6 M urea and supplemented with PhosSTOP® Phosphatase Inhibitor and cOmplete® EDTA-free Protease Inhibitor Cocktails (Roche). Reduced samples for SDS-PAGE were prepared in LDS sample buffer (Bio-Rad Laboratories) in the presence of 5% β-mercaptoethanol and incubated at room temperature for 1 h to reduce disulfide bonds. Non-reduced samples were prepared in LDS sample buffer without β-mercaptoethanol.

Samples were resolved by SDS-PAGE in 4–20% Criterion TGX Stain-Free Precast Gels and transferred onto Immun-Blot® Low Fluorescence PVDF membranes (Bio-Rad Laboratories). Immunoblotting analysis was performed using primary rabbit polyclonal antibodies to K14 (PRB-155P, Covance), or primary mouse monoclonal antibodies to phosphoserine (clone 4A4, Millipore), followed by horseradish-peroxidase-conjugated goat anti-rabbit-IgG or goat anti-mouse-IgG antibodies (Jackson ImmunoResearch). Enhanced chemiluminescence (Clarity™ Western ECL, Bio-Rad Laboratories) was performed according to the manufacturer's instructions. Protein bands were detected using a ChemiDoc Touch Imaging System (Bio-Rad Laboratories).

Statistical analysis

All data were analysed by one- or two-factor ANOVA and Tukey's test for post-hoc analysis. Significance was taken as $P<0.05$.

Acknowledgements

We would like to the thank Derek Warren (King's College London) for providing the DN-KASH constructs. We would also like to thank Arnoud Sonnenberg for providing the anti-nesprin-3 antibody and Patricia Costa for assistance with the dynamically adhesive micro-patterns.

Competing interests

The authors declare no competing or financial interests.

Author contributions

F.V.A. designed and carried out experiments and co-wrote the manuscript. G. Walko and G. Wiche generated the *Plec*-KO mice and cell lines and advised on experimental design. J.R.M. and J.A.M. provided EBS-MD skin samples and assisted with the analysis. A.H.B. advised on experimental design and data analysis. J.T.C. supervised the project, carried out experiments and co-wrote the manuscript.

Funding

This work was funded by the Biotechnology and Biological Sciences Research Council (BBSRC) [grant number BB/J000914/1]; and by the Barts and the London Charity [grant number 442/1032].

Supplementary information

Supplementary information available online at
http://jcs.biologists.org/lookup/suppl/doi:10.1242/jcs.173435/-/DC1

References

Andrä, K., Kornacker, I., Jörgl, A., Zörer, M., Spazierer, D., Fuchs, P., Fischer, I. and Wiche, G. (2003). Plectin-isoform-specific rescue of hemidesmosomal defects in plectin (–/–) keratinocytes. *J. Invest. Dermatol.* **120**, 189-197.

Bchetnia, M., Tremblay, M.-L., Leclerc, G., Dupérée, A., Powell, J., McCuaig, C., Morin, C., Legendre-Guillemin, V. and Laprise, C. (2012). Expression signature of epidermolysis bullosa simplex. *Hum. Genet.* **131**, 393-406.

Boczonadi, V., McInroy, L. and Määttä, A. (2007). Cytolinker cross-talk: periplakin N-terminus interacts with plectin to regulate keratin organisation and epithelial migration. *Exp. Cell Res.* **313**, 3579-3591.

Bonne, G., Di Barletta, M. R., Varnous, S., Becane, H. M., Hammouda, E.-H., Merlini, L., Muntoni, F., Greenberg, C. R., Gary, F., Urtizberea, J.-A. et al. (1999). Mutations in the gene encoding lamin A/C cause autosomal dominant Emery-Dreifuss muscular dystrophy. *Nat. Genet.* **21**, 285-288.

Botchkarev, V. A., Gdula, M. R., Mardaryev, A. N., Sharov, A. A. and Fessing, M. Y. (2012). Epigenetic regulation of gene expression in keratinocytes. *J. Invest. Dermatol.* **132**, 2505-2521.

Burgstaller, G., Gregor, M., Winter, L. and Wiche, G. (2010). Keeping the vimentin network under control: cell-matrix adhesion-associated plectin 1f affects cell shape and polarity of fibroblasts. *Mol. Biol. Cell* **21**, 3362-3375.

Busch, T., Armacki, M., Eiseler, T., Joodi, G., Temme, C., Jansen, J., Von Wichert, G., Omary, M. B., Spatz, J. and Seufferlein, T. (2012). Keratin 8 phosphorylation regulates keratin reorganization and migration of epithelial tumor cells. *J. Cell Sci.* **125**, 2148-2159.

Castañón, M. J., Walko, G., Winter, L. and Wiche, G. (2013). Plectin–intermediate filament partnership in skin, skeletal muscle, and peripheral nerve. *Histochem. Cell Biol.* **140**, 33-53.

Chalut, K. J., Höpfler, M., Lautenschläger, F., Boyde, L., Chan, C. J., Ekpenyong, A., Martinez-Arias, A. and Guck, J. (2012). Chromatin decondensation and nuclear softening accompany Nanog downregulation in embryonic stem cells. *Biophys. J.* **103**, 2060-2070.

Chen, C. S., Mrksich, M., Huang, S., Whitesides, G. M. and Ingber, D. E. (1997). Geometric control of cell life and death. *Science* **276**, 1425-1428.
Connelly, J. T., Gautrot, J. E., Trappmann, B., Tan, D. W.-M., Donati, G., Huck, W. T. S. and Watt, F. M. (2010). Actin and serum response factor transduce physical cues from the microenvironment to regulate epidermal stem cell fate decisions. *Nat. Cell Biol.* **12**, 711-718.
Connelly, J. T., Mishra, A., Gautrot, J. E. and Watt, F. M. (2011). Shape-induced terminal differentiation of human epidermal stem cells requires p38 and is regulated by histone acetylation. *PLoS ONE* **6**, e27259.
Costa, P., Gautrot, J. E. and Connelly, J. T. (2014). Directing cell migration using micropatterned and dynamically adhesive polymer brushes. *Acta Biomater.* **10**, 2415-2422.
Coulombe, P. A., Hutton, M. E., Letal, A., Hebert, A., Paller, A. S. and Fuchs, E. (1991). Point mutations in human keratin 14 genes of epidermolysis bullosa simplex patients: genetic and functional analyses. *Cell* **66**, 1301-1311.
Dupont, S., Morsut, L., Aragona, M., Enzo, E., Giulitti, S., Cordenonsi, M., Zanconato, F., Le Digabel, J., Forcato, M., Bicciato, S. et al. (2011). Role of YAP/TAZ in mechanotransduction. *Nature* **474**, 179-183.
Engler, A. J., Sen, S., Sweeney, H. L. and Discher, D. E. (2006). Matrix elasticity directs stem cell lineage specification. *Cell* **126**, 677-689.
Ezhkova, E., Pasolli, H. A., Parker, J. S., Stokes, N., Su, I.-h., Hannon, G., Tarakhovsky, A. and Fuchs, E. (2009). Ezh2 orchestrates gene expression for the stepwise differentiation of tissue-specific stem cells. *Cell* **136**, 1122-1135.
Feng, X. and Coulombe, P. A. (2015). A role for disulfide bonding in keratin intermediate filament organization and dynamics in skin keratinocytes. *J. Cell Biol.* **209**, 59-72.
Fessing, M. Y., Mardaryev, A. N., Gdula, M. R., Sharov, A. A., Sharova, T. Y., Rapisarda, V., Gordon, K. B., Smorodchenko, A. D., Poterlowicz, K., Ferone, G. et al. (2011). p63 regulates Satb1 to control tissue-specific chromatin remodeling during development of the epidermis. *J. Cell Biol.* **194**, 825-839.
Gdula, M. R., Poterlowicz, K., Mardaryev, A. N., Sharov, A. A., Peng, Y., Fessing, M. Y. and Botchkarev, V. A. (2013). Remodeling of three-dimensional organization of the nucleus during terminal keratinocyte differentiation in the epidermis. *J. Invest. Dermatol.* **133**, 2191-2201.
Goldman, R. D., Shumaker, D. K., Erdos, M. R., Eriksson, M., Goldman, A. E., Gordon, L. B., Gruenbaum, Y., Khuon, S., Mendez, M., Varga, R. et al. (2004). Accumulation of mutant lamin A causes progressive changes in nuclear architecture in Hutchinson-Gilford progeria syndrome. *Proc. Natl. Acad. Sci. USA* **101**, 8963-8968.
Gregor, M., Osmanagic-Myers, S., Burgstaller, G., Wolfram, M., Fischer, I., Walko, G., Resch, G. P., Jörgl, A., Herrmann, H. and Wiche, G. (2014). Mechanosensing through focal adhesion-anchored intermediate filaments. *FASEB J.* **28**, 715-729.
Guilluy, C., Osborne, L. D., Van Landeghem, L., Sharek, L., Superfine, R., Garcia-Mata, R. and Burridge, K. (2014). Isolated nuclei adapt to force and reveal a mechanotransduction pathway in the nucleus. *Nat. Cell Biol.* **16**, 376-381.
Gundersen, G. G. and Worman, H. J. (2013). Nuclear positioning. *Cell* **152**, 1376-1389.
Hale, C. M., Shrestha, A. L., Khatau, S. B., Stewart-Hutchinson, P. J., Hernandez, L., Stewart, C. L., Hodzic, D. and Wirtz, D. (2008). Dysfunctional connections between the nucleus and the actin and microtubule networks in laminopathic models. *Biophys. J.* **95**, 5462-5475.
Horn, H. F., Brownstein, Z., Lenz, D. R., Shivatzki, S., Dror, A. A., Dagan-Rosenfeld, O., Friedman, L. M., Roux, K. J., Kozlov, S., Jeang, K.-T. et al. (2013). The LINC complex is essential for hearing. *J. Clin. Invest.* **123**, 740-750.
Isermann, P. and Lammerding, J. (2013). Nuclear mechanics and mechanotransduction in health and disease. *Curr. Biol.* **23**, R1113-R1121.
Iyer, K. V., Pulford, S., Mogilner, A. and Shivashankar, G. V. (2012). Mechanical activation of cells induces chromatin remodeling preceding MKL nuclear transport. *Biophys. J.* **103**, 1416-1428.
Ketema, M., Kreft, M., Secades, P., Janssen, H. and Sonnenberg, A. (2013). Nesprin-3 connects plectin and vimentin to the nuclear envelope of Sertoli cells but is not required for Sertoli cell function in spermatogenesis. *Mol. Biol. Cell* **24**, 2454-2466.
Khatau, S. B., Bloom, R. J., Bajpai, S., Razafsky, D., Zang, S., Giri, A., Wu, P.-H., Marchand, J., Celedon, A., Hale, C. M. et al. (2012). The distinct roles of the nucleus and nucleus-cytoskeleton connections in three-dimensional cell migration. *Sci. Rep.* **2**, 488.
Kovács, M., Tóth, J., Hetényi, C., Málnási-Csizmadia, A. and Sellers, J. R. (2004). Mechanism of blebbistatin inhibition of myosin II. *J. Biol. Chem.* **279**, 35557-35563.
Kröger, C., Loschke, F., Schwarz, N., Windoffer, R., Leube, R. E. and Magin, T. M. (2013). Keratins control intercellular adhesion involving PKC-α-mediated desmoplakin phosphorylation. *J. Cell Biol.* **201**, 681-692.
Lammerding, J., Schulze, P. C., Takahashi, T., Kozlov, S., Sullivan, T., Kamm, R. D., Stewart, C. L. and Lee, R. T. (2004). Lamin A/C deficiency causes defective nuclear mechanics and mechanotransduction. *J. Clin. Invest.* **113**, 370-378.
Lee, J. S. H., Hale, C. M., Panorchan, P., Khatau, S. B., George, J. P., Tseng, Y., Stewart, C. L., Hodzic, D. and Wirtz, D. (2007). Nuclear lamin A/C deficiency induces defects in cell mechanics, polarization, and migration. *Biophys. J.* **93**, 2542-2552.
Lee, C.-H., Kim, M.-S., Chung, B. M., Leahy, D. J. and Coulombe, P. A. (2012). Structural basis for heteromeric assembly and perinuclear organization of keratin filaments. *Nat. Struct. Mol. Biol.* **19**, 707-715.
Li, Q., Kumar, A., Makhija, E. and Shivashankar, G. V. (2014). The regulation of dynamic mechanical coupling between actin cytoskeleton and nucleus by matrix geometry. *Biomaterials* **35**, 961-969.
Lu, H., Chen, J., Planko, L., Zigrino, P., Klein-Hitpass, L. and Magin, T. M. (2007). Induction of inflammatory cytokines by a keratin mutation and their repression by a small molecule in a mouse model for EBS. *J. Invest. Dermatol.* **127**, 2781-2789.
Mardaryev, A. N., Gdula, M. R., Yarker, J. L., Emelianov, V. N., Poterlowicz, K., Sharov, A. A., Sharova, T. Y., Scarpa, J. A., Chambon, P., Botchkarev, V. A. et al. (2014). p63 and Brg1 control developmentally regulated higher-order chromatin remodelling at the epidermal differentiation complex locus in epidermal progenitor cells. *Development* **141**, 101-111.
McBeath, R., Pirone, D. M., Nelson, C. M., Bhadriraju, K. and Chen, C. S. (2004). Cell shape, cytoskeletal tension, and RhoA regulate stem cell lineage commitment. *Dev. Cell* **6**, 483-495.
McLean, W. H., Pulkkinen, L., Smith, F. J., Rugg, E. L., Lane, E. B., Bullrich, F., Burgeson, R. E., Amano, S., Hudson, D. L., Owaribe, K., et al. (1996). Loss of plectin causes epidermolysis bullosa with muscular dystrophy: cDNA cloning and genomic organization. *Genes Dev.* **10**, 1724-1735.
Moll, R., Franke, W. W., Schiller, D. L., Geiger, B. and Krepler, R. (1982). The catalog of human cytokeratins: patterns of expression in normal epithelia, tumors and cultured cells. *Cell* **31**, 11-24.
Na, S., Chowdhury, F., Tay, B., Ouyang, M., Gregor, M., Wang, Y., Wiche, G. and Wang, N. (2009). Plectin contributes to mechanical properties of living cells. *Am. J. Physiol. Cell Physiol.* **296**, C868-C877.
Osmanagic-Myers, S., Gregor, M., Walko, G., Burgstaller, G., Reipert, S. and Wiche, G. (2006). Plectin-controlled keratin cytoarchitecture affects MAP kinases involved in cellular stress response and migration. *J. Cell Biol.* **174**, 557-568.
Paszek, M. J., Zahir, N., Johnson, K. R., Lakins, J. N., Rozenberg, G. I., Gefen, A., Reinhart-King, C. A., Margulies, S. S., Dembo, M., Boettiger, D. et al. (2005). Tensional homeostasis and the malignant phenotype. *Cancer Cell* **8**, 241-254.
Pelham, R. J. and Wang, Y.-l. (1997). Cell locomotion and focal adhesions are regulated by substrate flexibility. *Proc. Natl. Acad. Sci. USA* **94**, 13661-13665.
Ramms, L., Fabris, G., Windoffer, R., Schwarz, N., Springer, R., Zhou, C., Lazar, J., Stiefel, S., Hersch, N., Schnakenberg, U. et al. (2013). Keratins as the main component for the mechanical integrity of keratinocytes. *Proc. Natl. Acad. Sci. USA* **110**, 18513-18518.
Reyes, C. D. and García, A. J. (2003). Engineering integrin-specific surfaces with a triple-helical collagen-mimetic peptide. *J. Biomed. Mater. Res.* **65A**, 511-523.
Rezniczek, G. A., de Pereda, J. M., Reipert, S. and Wiche, G. (1998). Linking integrin alpha6beta4-based cell adhesion to the intermediate filament cytoskeleton: direct interaction between the beta4 subunit and plectin at multiple molecular sites. *J. Cell Biol.* **141**, 209-225.
Rheinwald, J. G. and Green, H. (1977). Epidermal growth factor and the multiplication of cultured human epidermal keratinocytes. *Nature* **265**, 421-424.
Roux, K. J., Crisp, M. L., Liu, Q., Kim, D., Kozlov, S., Stewart, C. L. and Burke, B. (2009). Nesprin 4 is an outer nuclear membrane protein that can induce kinesin-mediated cell polarization. *Proc. Natl. Acad. Sci. USA* **106**, 2194-2199.
Russell, D., Andrews, P. D., James, J. and Lane, E. B. (2004). Mechanical stress induces profound remodelling of keratin filaments and cell junctions in epidermolysis bullosa simplex keratinocytes. *J. Cell Sci.* **117**, 5233-5243.
Sagelius, H., Rosengardten, Y., Hanif, M., Erdos, M. R., Rozell, B., Collins, F. S. and Eriksson, M. (2008). Targeted transgenic expression of the mutation causing Hutchinson-Gilford progeria syndrome leads to proliferative and degenerative epidermal disease. *J. Cell Sci.* **121**, 969-978.
Seltmann, K., Fritsch, A. W., Käs, J. A. and Magin, T. M. (2013). Keratins significantly contribute to cell stiffness and impact invasive behavior. *Proc. Natl. Acad. Sci. USA* **110**, 18507-18512.
Smith, F. J. D., Eady, R. A. J., Leigh, I. M., McMillan, J. R., Rugg, E. L., Kelsell, D. P., Bryant, S. P., Spurr, N. K., Geddes, J. F., Kirtschig, G. et al. (1996). Plectin deficiency results in muscular dystrophy with epidermolysis bullosa. *Nat. Genet.* **13**, 450-457.
Spurny, R., Gregor, M., Castañón, M. J. and Wiche, G. (2008). Plectin deficiency affects precursor formation and dynamics of vimentin networks. *Exp. Cell Res.* **314**, 3570-3580.
Starr, D. A. and Fridolfsson, H. N. (2010). Interactions between nuclei and the cytoskeleton are mediated by SUN-KASH nuclear-envelope bridges. *Annu. Rev. Cell Dev. Biol.* **26**, 421-444.
Steinböck, F. A., Nikolic, B., Coulombe, P. A., Fuchs, E., Traub, P. and Wiche, G. (2000). Dose-dependent linkage, assembly inhibition and disassembly of vimentin and cytokeratin 5/14 filaments through plectin's intermediate filament-binding domain. *J. Cell Sci.* **113**, 483-491.
Swift, J., Ivanovska, I. L., Buxboim, A., Harada, T., Dingal, P. C. D. P., Pinter, J., Pajerowski, J. D., Spinler, K. R., Shin, J.-W., Tewari, M. et al. (2013). Nuclear

lamin-A scales with tissue stiffness and enhances matrix-directed differentiation. *Science* **341**, 1240104.

Tian, R., Gregor, M., Wiche, G. and Goldman, J. E. (2006). Plectin regulates the organization of glial fibrillary acidic protein in Alexander disease. *Am. J. Pathol.* **168**, 888-897.

Toivola, D. M., Zhou, Q., English, L. S. and Omary, M. B. (2002). Type II keratins are phosphorylated on a unique motif during stress and mitosis in tissues and cultured cells. *Mol. Biol. Cell* **13**, 1857-1870.

Versaevel, M., Grevesse, T. and Gabriele, S. (2012). Spatial coordination between cell and nuclear shape within micropatterned endothelial cells. *Nat. Commun.* **3**, 671.

Walko, G., Vukasinovic, N., Gross, K., Fischer, I., Sibitz, S., Fuchs, P., Reipert, S., Jungwirth, U., Berger, W., Salzer, U. et al. (2011). Targeted proteolysis of plectin isoform 1a accounts for hemidesmosome dysfunction in mice mimicking the dominant skin blistering disease EBS-Ogna. *PLoS Genet.* **7**, e1002396.

Wang, Y., Panteleyev, A. A., Owens, D. M., Djabali, K., Stewart, C. L. and Worman, H. J. (2008). Epidermal expression of the truncated prelamin A causing Hutchinson-Gilford progeria syndrome: effects on keratinocytes, hair and skin. *Hum. Mol. Genet.* **17**, 2357-2369.

Wilhelmsen, K., Litjens, S. H., Kuikman, I., Tshimbalanga, N., Janssen, H., Van den Bout, I., Raymond, K. and Sonnenberg, A. (2005). Nesprin-3, a novel outer nuclear membrane protein, associates with the cytoskeletal linker protein plectin. *J. Cell Biol.* **171**, 799-810.

Winter, L. and Wiche, G. (2013). The many faces of plectin and plectinopathies: pathology and mechanisms. *Acta Neuropathol.* **125**, 77-93.

Zhang, Q., Skepper, J. N., Yang, F., Davies, J. D., Hegyi, L., Roberts, R. G., Weissberg, P. L., Ellis, J. A. and Shanahan, C. M. (2001). Nesprins: a novel family of spectrin-repeat-containing proteins that localize to the nuclear membrane in multiple tissues. *J. Cell Sci.* **114**, 4485-4498.

Zhang, X., Lei, K., Yuan, X., Wu, X., Zhuang, Y., Xu, T., Xu, R. and Han, M. (2009). SUN1/2 and Syne/Nesprin-1/2 complexes connect centrosome to the nucleus during neurogenesis and neuronal migration in mice. *Neuron* **64**, 173-187.

Zhen, Y.-Y., Libotte, T., Munck, M., Noegel, A. A. and Korenbaum, E. (2002). NUANCE, a giant protein connecting the nucleus and actin cytoskeleton. *J. Cell Sci.* **115**, 3207-3222.

Journal of Cell Science

Supplementary Figures

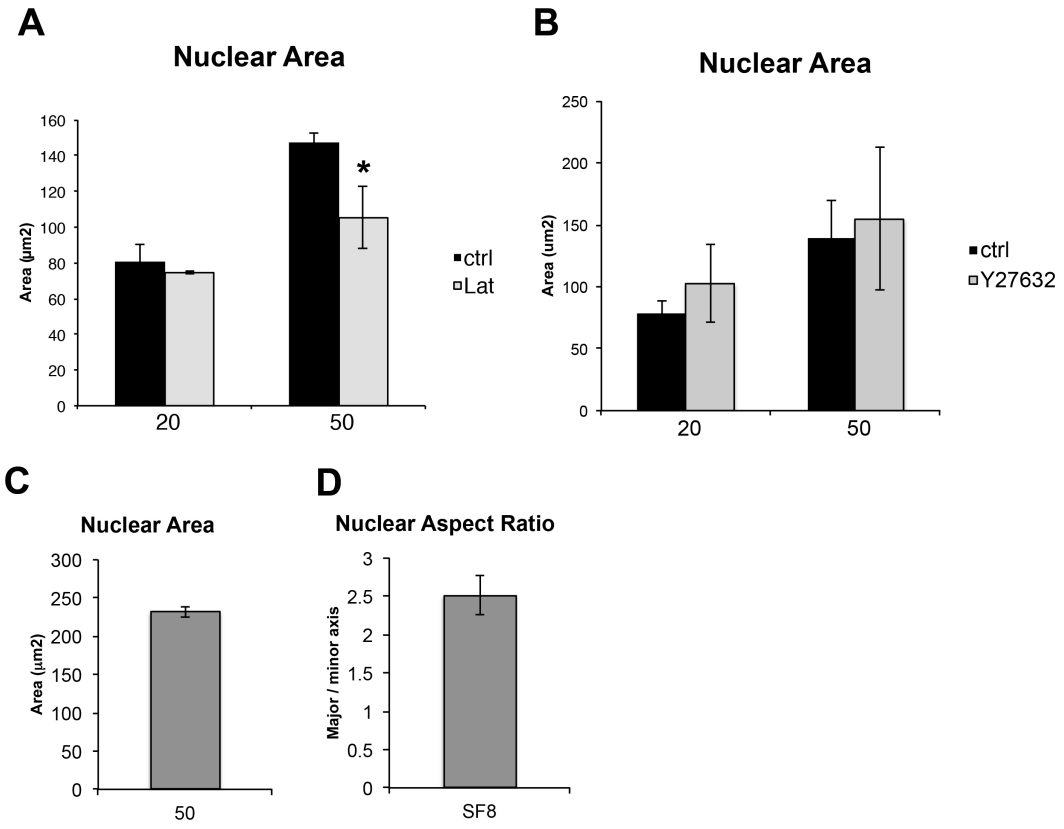

Figure S1: Quantification of nuclear morphology of human keratinocytes and HeLa cells on micro-patterned substrates. (A) Quantification of nuclear area of primary human keratinocytes on 20 μm and 50 μm islands following treatment with 1 μM Latrunculin A or (B) 10 μM Y27632. Data represent mean ± SEM (N=3 experiments). *P<0.05 compared to carrier control (0.1% DMSO). (C) Quantification of nuclear cross-sectional area of HeLa cells on 50 μm islands and (D) aspect ration on SF8 islands. Data represent mean ± SEM (N=3 experiments).

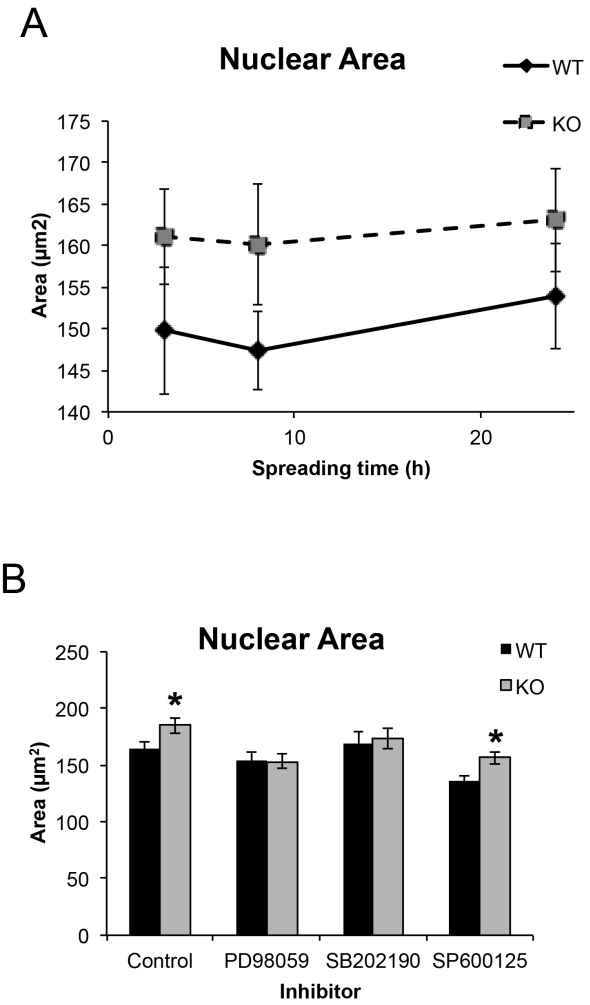

Figure S2: Stability and MAPK dependence of Plec-induced nuclear deformation: (A) WT and Plec KO keratinocytes were seeded on 50 μm substrates, and nuclear morphology was analysed at 4, 8, and 24 hours after seeding. Quantification of nuclear cross-sectional area in DAPI stained cells was performed using ImageJ. Data represent mean ± SEM (n=30 cells). (B) Nuclear cross-sectional area was quantified in WT and KO cells culture on 50 μm islands for 4 hours in the absence (0.1% DMSO) or presence of MAPK inhibitors, 10 μM PD98059 (Erk1/2), 2 μM SB202190 (p38), and 10 μM SP600125 (Jnk). *P<0.05 compared to WT. Data represent mean ± SEM (n=30 cells).

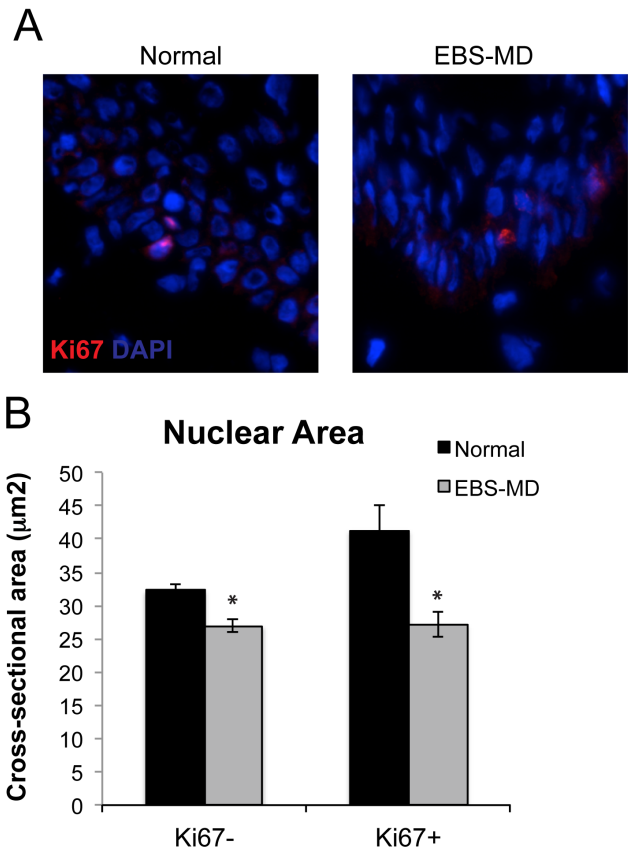

Figure S3: Nuclear morphology in proliferative and non-proliferative cells. (A) Representative immunofluorescence images of normal and plectin deficient, EBS-MD, skin stained for Ki67. (B) Quantification of nuclear cross-sectional area for Ki67 positive and negative cells in normal and EBS-MD skin. Data represent mean ± SEM (n=30 cells). *P < 0.05 compared to Normal.

Table S1: Details of gender, age, and anatomical location of human skin samples

Sample ID	Gender/Age	Location
EB1	M/neonate	Arm
EB2	M/neonate	Thigh
EB3	M/16 years	Arm
EB4	F/7 months	Thigh
Normal 1	M/neonate	Foreskin
Normal 2	M/neonate	Foreskin
Normal 3	F/36	Abdomen
Normal 4	F/47	Abdomen